VERTICAL SEAWALLS PROTECTED BY RUBBLE MOUND STRUCTURES: PREDICTION TOOLS AND PHYSICAL INSIGHT

Sara Tuozzo[1], Angela Di Leo[2], Margherita Carmen Ciccaglione[1], Fabio Dentale[2], Luis Cordova Lopez[3], Mario Calabrese[1] and Mariano Buccino[1]

The role of adaptive solutions for reducing coastal risks is a crucial issue that is increasingly captivating the coastal community. The present work analyzes attached/detached rubble mound breakwaters designed to protect vertical walls with very shallow foreshores. In particular, we aim to understand the behavior of these protective structures in reducing wave overtopping at seawalls and, thus, softening flooding risks. Laboratory data and CFD numerical experiments have shown that these adaptive solutions have a beneficial effect as long as the seawall is not located in the inner surf zone. Finally, we have provided mean overtopping discharge predictive tools for walls protected by either attached or detached breakwaters.

Keywords: wave overtopping; rubble-mound breakwaters; physical model experiments; CFD numerical experiments

INTRODUCTION

Coastal engineers are facing new challenges in designing sea defenses to mitigate the flooding risk of coastal areas, especially because of the sea level rise expectations. Particularly, adaptive solutions that increase the protective capability of classic defense structures are increasingly engaging coastal scientific and engineering communities (e.g. Salauddin et al., 2021; Dong et al., 2021; Pratola et al., 2021). Moreover, the literature recently focuses on sea defenses located under depth-limited conditions, as the sea level rise might increase the wave loadings at the structure (Van Gent, 2024; Mata and Van Gent, 2023).

There are different types of adaptive solutions, which can be distinguished according to their effect. Solutions that consist of modifying the structure shape (such as designing a recurved wall or introducing a berm in the seaward slope) act by increasing the dissipation on the structure; on the other hand, some solutions attempt to act by dissipating energy before waves reach the structure (e.g., introducing a beach nourishment or a rubble mound breakwater in front of the existing structure). Nonetheless, in contrast to the former group, a few works have dealt with the second type of adaptive structures.

In this work, we have analyzed seawalls protected by rubble mound breakwaters, either attached or detached. Specifically, we have investigated their effect in reducing wave overtopping. The analysis encompasses laboratory and numerical experiments. Indeed, numerical models represent nowadays a valid instrument for accurately studying wave effects on both beaches and man-made-structures (Mata and Van Gent, 2023; Di Leo et al., 2022a,b; Chen et al., 2022; Castellino et al., 2021; Buccino et al., 2021; Di Leo et al., 2017). Laboratory data have been derived from a broad physical experimental campaign conducted at the University of Naples Federico II (Lopez et al., 2016; 2015) to examine the wave overtopping at the Malecòn vertical wall of La Havana city (Cuba). On the other hand, numerical experiments have been performed using the CFD model FLOW-3D (Flow Science, Inc., 2009). In particular, we have adopted the RANS/VOF innovative procedure of Dentale et al. (2014a,b) to model the rubble mounds instead of the simplified modelling of porous structures (e.g. Higuera et al., 2014).

The work first aims to understand the behavior of vertical walls in very shallow water protected by rubble mound breakwaters and, then, tries to evaluate their performance in decreasing wave overtopping. Indeed, the literature review has highlighted the paucity of adequate tools for estimating the flow rate reduction. Finally, the work provides empirical design tools for predicting the mean overtopping discharge of vertical seawalls protected by either attached or detached breakwaters.

PHYSICAL EXPERIMENTAL CAMPAIGN

In this work, we analyze the laboratory data carried out at the University of Naples Federico II (Lopez et al. 2015; 2016) to investigate the wave overtopping at the Malecòn Tradizionàl, which is the vertical seawall that protect La Havana city (Cuba) against flooding. Specifically, the Malecòn vertical wall and other several design variants were examined in order to individuate the configuration that would reduce the mean overtopping discharge. The variants encompass increasing the crest freeboard, modifying the wall's profile (i.e. recurved wall) and introducing coastal protective structures, such as rock rubble mounds or low-crested detached breakwaters. Among the 360 tests, we handle 116 experiments that deal with either the seawall protected by rubble mound breakwaters (*S-RMB*) or the seawall protected by low-

[1] University of Naples Federico II, Italy

[2] University of Salerno, Italy

[3] Universidad Tecnológica de La Habana José Antonio Echeverría, Cuba

crested breakwaters (*S-LCB*). Moreover, the Malecòn original configuration (i.e., the unprotected seawall, *US*) tests have been used to evaluate the protective degree provided by the attached/detached breakwaters.

The experiments were carried out in a flume long 18.4m and wide 1.55m. The multi-slope Havana foreshore (Fig. 1a) and the several sea defences were modelled according to the Froude similitude law using the lengthscale ratio of $\lambda = 30$.

Two surge values were simulated, namely + 1.73m and +2.28m (in prototype) above the SWL (Fig. 1b). The former corresponds to a return period of 50 years, whereas the latter reproduces the water level measured in 2005 under hurricane Wilma. For each surge eight random wave sea states described by the mean JONSWAP spectrum were tested; these generated sea states are characterized by four significant wave heights (H_{m0} = 2.7m, 4.0m, 5.4m and 6.5m) and two peak periods (T_p = 10s and 12s). According to the values of $h_{TOE}/H_{m0,deep}$ (i.e., Hofland et al. 2017 classification), the Malecòn seawall is located in shallow and very shallow water.

It is worth noting that the incoming wave conditions (i.e. wave characteristics measured at the toe of the structures) were obtained running the sea-states for 200 waves without any structure in the flume; on the other hand, the sea-states were run for 1000 waves to measure the mean overtopping discharge.

Further details of the physical experimental campaign can be found in Buccino et al. (2023), Lopez et al. (2015, 2016).

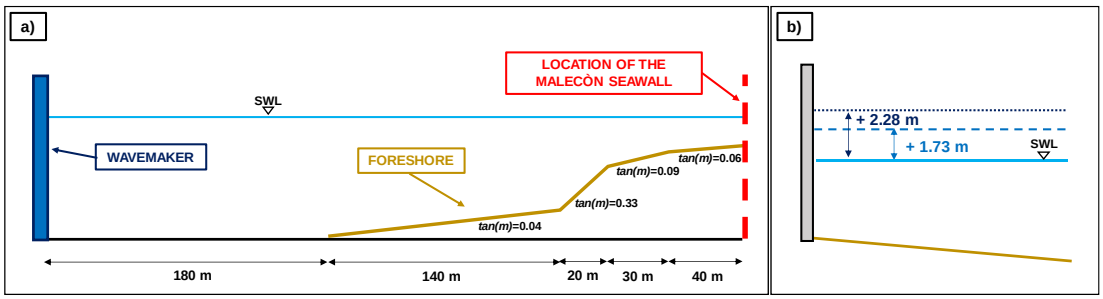

Figure 1. Sketch of the physical model: panel a) shows the multi-slope Havana foreshore, while panel b) depicts the two surge values investigated. Prototype values are reported.

S-RMB experiments

The first configuration concerns the vertical wall protected by rubble mound breakwaters (Fig. 2a and 2b). In particular, the 36 laboratory data have been gathered using three different layouts that vary both in crest width, G_C, and crest freeboard, A_C, while the off-shore slope α_{off} was kept constant (Table 1). Clearly, using two levels of surge allowed us to analyze emerged, submerged and zero-freeboard rubble mound breakwaters. As schematize in Fig. 2a, the structures had no core; they are composed by a median rock size equal to 1.0m in prototype scale. The displacement of rocks was avoided by securing each structure with a steel grid.

Table 1. Main geometrical features of the rubble mound breakwaters reported in prototype scale.

	αoff [-]	G_C [m]	A_C [m]
RMB 1	2/3	5.0	+3.28
RMB 2	2/3	20.0	+2.28
RMB 3	2/3	30.0	+1.73

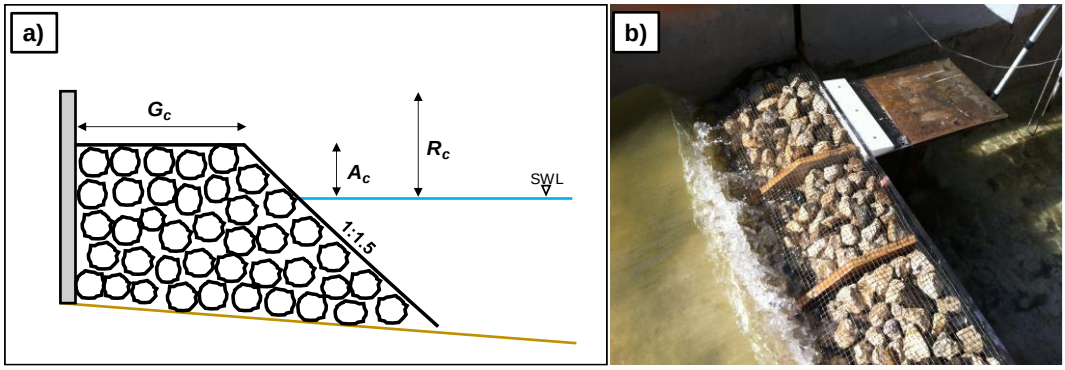

Figure 2. Vertical seawall protected by rubble mound breakwaters. Panel a) depicts the sketch of the RBMs investigated, while panel b) shows *RMB 1* modelled in the physical experimental campaign.

S-LCB experiments

The second configuration consists in the vertical seawall protected by detached low-crested breakwaters (Figs. 3a and 3b). For this group of experiments (64 laboratory tests), four LCBs were modelled; in particular, both the crest width and freeboard were varied, while both the off-shore and leeward slopes had a fixed value of 2/3, as reported in Table 2. Analogously to the RMBs, the two water levels tested ensured to investigate the protection degree of emerged, submerged and zero-freeboard structures. The four layouts were placed at the same water depth at the seaward toe, *h*, and, thus, are characterized by a different distance, *X*, from the seawall (Table 2). Fig. 3d shows that the low-crested breakwaters were constituted by a core which is protected by an armor of rocks with a median diameter of 1.46m in prototype. Since in this work we do not take into account the hydraulic stability, we only consider the experiments performed with a steel grid that avoid the stones' displacements.

Furthermore, Figs. 3a and 3b highlight that the structures were built raised above the floor to avoid the piling-up phenomenon (see Calabrese et al., 2008).

Table 2. Main geometrical features of the low-crested breakwaters reported in prototype scale.

	α [-]	G_C [m]	A_C [m]	h [m]	X [m]
LCB 1	2/3	30.0	-0.2	5.05	16.44
LCB 2	2/3	30.0	+0.54	5.05	16.44
LCB 3	2/3	22.0	+2.28	5.05	16.98
LCB 4	2/3	12.0	+3.28	5.05	23.53

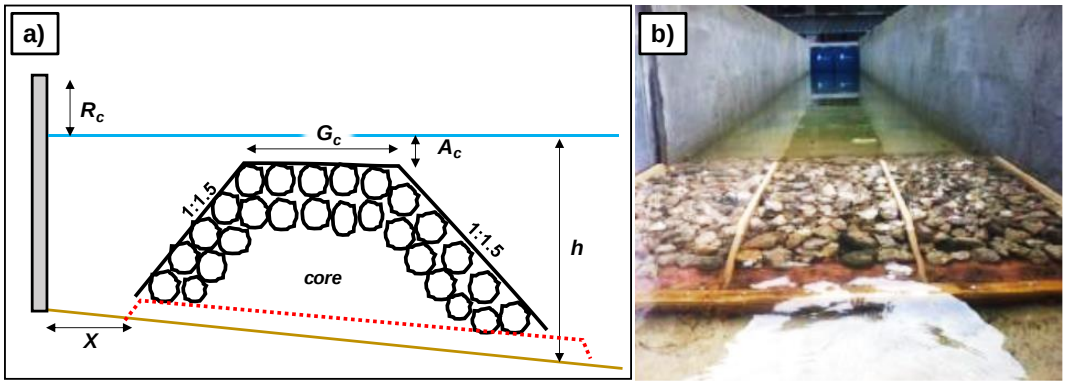

Figure 3. Vertical seawall protected by low-crested breakwaters. Panel a) depicts the sketch of the LCBs investigated, while panel b) shows *LCB 3* modelled in the physical experimental campaign.

NUMERICAL EXPERIMENTS

To better understand the capability of these protective structures in reducing wave overtopping, we resort to numerical modelling. In particular, we perform some numerical tests that reproduce – at the prototype scale – seawalls protected by RMBs.

Numerical experiments have been carried out using FLOW-3D (Flow Science, Inc., 2009), which is a popular CFD software that integrates the Reynolds Averaged Navier-Stokes equations combined with the Volume of Fluid method to track the fluid surfaces.

The peculiarity of these tests consists in the numerical modelling of rubble mound breakwaters; indeed, we adopt the "microscopic approach" introduced by Dentale et al. (2014a,b) that integrates CAD and CFD software to reproduce precisely each element of the breakwaters (see Fig. 4). Such a technique allows to better analyzing the interaction between waves and porous structures.

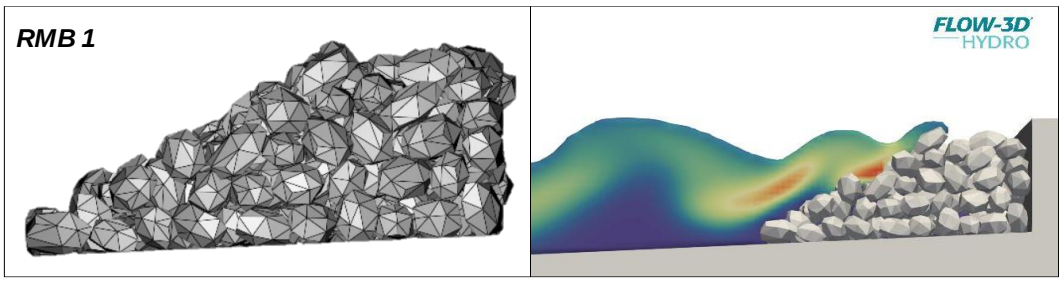

Figure 4. RMB modelled using the approach of Dentale et al. (2014a,b).

In the numerical analysis, we have tested the Malecòn seawall protected by the three RMBs of Table 1, using the lower water level (i.e. +1.73m above the SWL) in order to examine the shallower water conditions. The random sea states investigated are characterized by a range of significant wave heights that varies between 2.9m and 5.0m, and two peak periods (T_p = 10s and 12s).

The numerical domain, which is long 550m, height 40m and wide 3m, had been divided into sub-domains with different grid sizes, based on the mesh convergence study presented in Di Leo (2021). In particular, the mesh sizes are 0.6x0.6x0.6m in the flat portion of the domain and 0.40x0.40x0.40m along the multi-slope bottom (Fig. 5). Moreover, at the structure, the mesh size has been reduced to 0.3x0.3x0.3m. Fig.5 describes the adopted boundary conditions as well. Specifically, at the end of the flume "Outflow condition" allows the waves to leave the domain without any reflections, while, on the other side, "Pressure" guarantees a constant water level in the numerical flume. At the lateral and upper bounds, the "Symmetry boundaries" ensure that the velocity gradient vanishes and turbulence production is zero. Finally, a "Wall" condition at the bottom cancels out the velocity component normal to the seafloor. As depicted in the scheme of Fig. 5, the mass-source element has been used to generate the random waves (Lin et al., 1999); waves reflected by this solid are then dissipated by the sponge layer.

Finally, we have used the RNG k-ε model as turbulence closure.

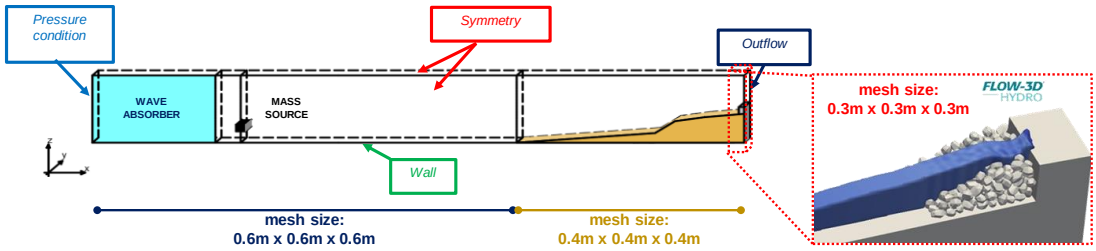

Figure 5. Scheme of the CFD computational domain.

AVAILABLE TOOLS

The first step of this work is to evaluate the existing formulae that engineers can use with these configurations and their performance in evaluating the mean overtopping discharge.

The state-of-the-art analysis highlights that we may adopt different tools for seawalls protected by rubble mound breakwaters, depending on whether the protective structures are emerged or submerged, while it is challenging to estimate the flow rate of seawalls protected by detached structures.

In particular, to the best of the authors' knowledge, Van Gent (2024) is the only work that dealt with the overtopping of structures protected by detached submerged low-crested breakwaters. However, the author has only suggested reducing the crest freeboard by the structure-induced wave set-up before applying the existing tools to estimate the mean flow rate. Therefore, it appears unsuitable for *S-LCB* data due to the experiments' layout; indeed, the structure-induced wave set-up has been avoided by

raising the LCBs (Figs. 3a and 3b). Hence, we cannot adopt any overtopping predictive formula for *S-LCB* experiments.

Concerning the S-RMB experiments, we need to distinguish between emerged, zero-freeboards and submerged rubble mounds and then apply different empirical tools. Specifically, the EurOtop manual 2018 suggests using the empirical formulae for composite vertical walls for submerged RMBs (Eq. 1), and adapting the prediction methods used for crown walls on an armoured rubble mound in case of emerged RMBs (Eqs. 2-3). Hence, for submerged RMBs we use the following formula:

$$q_{COMPOSITEWALL} = 1.3\sqrt{\frac{d}{h}} \cdot q_{VERTICALWALL} \qquad (1)$$

where d indicates the submergence of the rubble mound and h is the water depth at the toe of the structure.

On the other hand, for emerged/zero freeboard RMBs we adopt:

$$\frac{q}{\sqrt{gH_{m0}^3}} = 0.09\exp\left[-\left(1.5\frac{R_C}{H_{m0}\cdot\gamma_f}\right)^{1.3}\right] \qquad (2)$$

$$C_r = \max\left[1;3.06\exp\left(-1.5\frac{G_C}{H_{m0}}\right)\right] \qquad (3)$$

where H_{m0} is the incident wave height, γ_f is the roughness factor; R_C in Eq. 2 according to the EurOtop manual, is the maximum value between the crown wall's and the rubble mound's freeboard. Moreover, the reducing factor in Eq. 3 is applied when the crest width G_C is larger than $3D_{n,50}$.

It is worth pointing out that the EurOtop manual indicates the EurOtop Artificial Neural Network (ANN) developed by Zanuttigh et al. (2016) as an alternative tool.

Recently, Van Gent et al. (2022) and Mata and Van Gent (2023) performed both a physical and a numerical experimental campaign to investigate the overtopping of emerged rubble mound breakwaters with a crown wall. The following overtopping predictive model has been provided:

$$\frac{q}{\sqrt{gH_{m0}^3}} = \frac{0.03}{\sqrt{s_{m-10}}}\cdot\cot\alpha_{OFF}\cdot\exp\left[-\frac{4\cdot R_C}{\gamma_f\cdot\gamma_v\cdot\gamma_b\cdot H_{m0}\cdot\xi_{m-10}^{0.5}}\right] \qquad (4)$$

where the wave steepness s_{m-10} and the surf-similarity parameter ξ_{m-10} are determined using the harmonic spectral period, T_{m-10}, and the wave height, H_{m0}, at the toe of the structure; R_C is the crest freeboard of the crown wall and α_{off} is the offshore slope of the rubble mound breakwater. For the three reduction coefficients, the authors proposed the following formulae:

$$\gamma_f = 1-0.7\left(\frac{D_{n,50}}{H_{m0}}\right)^{0.1} \qquad (5)$$

$$\gamma_v = 1+0.45\left(\frac{R_C-A_C}{R_C}\right) \qquad (6)$$

$$\gamma_b = 1-8\left(\frac{s_{m-10}\cdot B}{H_{m0}}\right)\left(1-0.36\left[\frac{B_L}{s_{m-10}\cdot A_C}\right]^{0.15}\right) \qquad (7)$$

where the roughness factor γ_f depends explicitly on the stone's diameter, while γ_v and γ_b account for the influence of the crest wall and the berm, respectively. In particular, the latter considers both the berm width, B, and its vertical distance from the crest of the rubble mound, B_L.

To verify the capabilities of these existing models in predicting the mean overtopping discharge, we compare the computed and estimated q of the S-RMB experiments. Specifically, Fig. 6 shows the overtopping models' performances distinguishing between emerged, submerged and zero-freeboard RMBs. It is worth noticing that the Mata and Van Gent model (Eqs. 4-7) has been employed only for emerged structures.

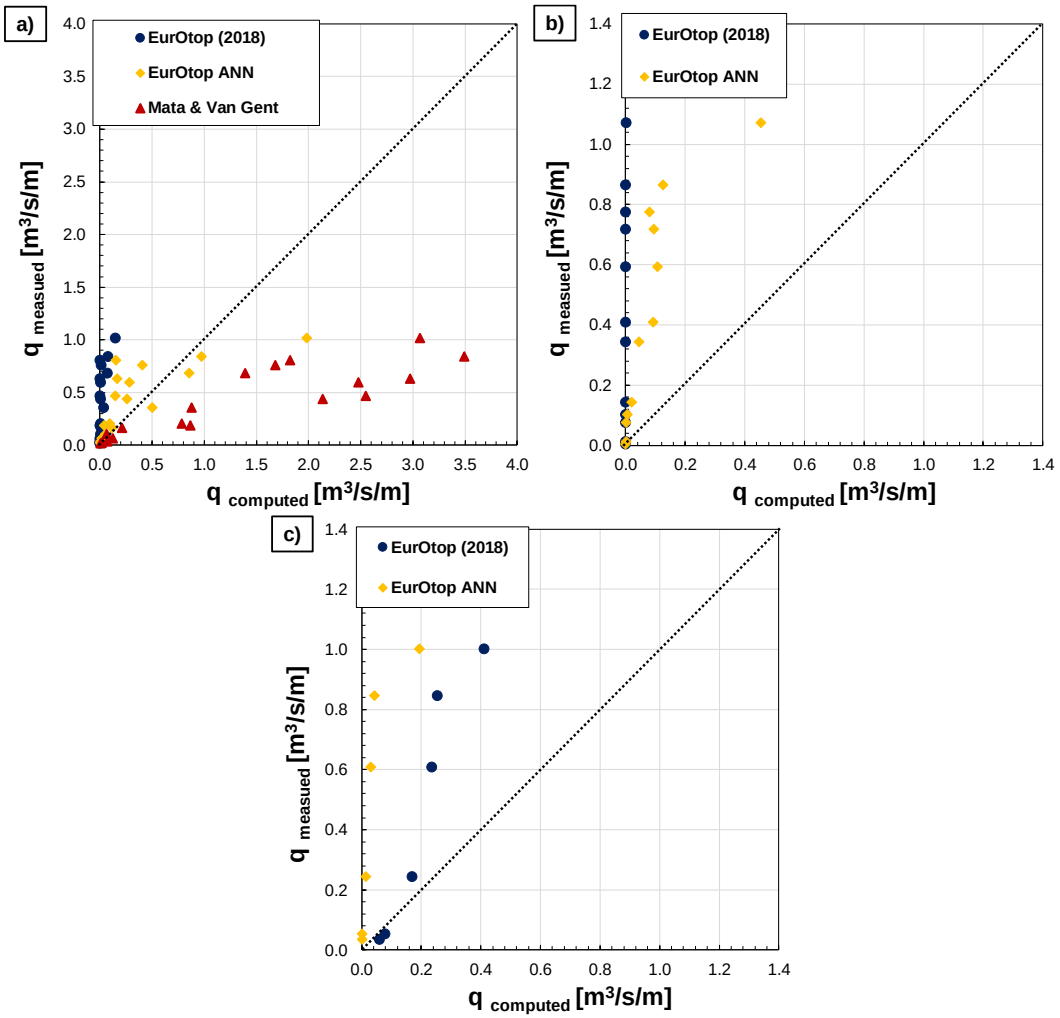

Figure 6. Comparison between measured and computed mean overtopping discharge of S-RMBs: panel a) refers to emerged structures, while panel b) and panel c) refer to zero-freeboard and submerged rubble mounds, respectively. The black dotted line indicates the perfect agreement.

The comparison shows that the EurOtop formulae (Eqs. 1-3) and the ANN tend to underestimate the flow rate; in particular, the former provides larger underestimations for emerged/zero-freeboard RMBs (Figs. 6a and 6b), while the ANN has the worst performance with the submerged structures (Fig. 6c). On the other hand, the overtopping model of Mata and Van Gent overestimates q, especially for the larger flow rates (Fig. 6a).

Overall, these results clearly indicate a poor agreement between measurements and estimates, regardless of the empirical model used. Therefore, the existing predictive tools appear inadequate to predict the mean overtopping discharge of seawalls in very shallow water protected by rubble mound breakwaters. Contemporary, the literature has not yet provided a model to estimate the flow rate of seawalls protected by low-crested breakwaters.

Hence, this paucity of adequate existing tools points out the necessity of deriving a reliable model that predicts the q reduction capacity of these two different protective structures.

RESULTS

The assessment of existing empirical tools reveals our inability to easily predict how attached/detached rubble mound structures may reduce the mean overtopping discharge at vertical walls in shallow water. Therefore, in this Section, we try to overcome such a limitation and provide tentative empirical formulae.

Influence of protective structures on wave overtopping

We aim to evaluate the flow rate reduction at vertical seawalls due to the presence of either attached or detached rubble mound breakwaters. Such a reduction is expressed via the wave overtopping reduction ratio, C_q:

$$C_q = \frac{q_{PROTECTEDWALL}}{q_{UNPROTECTEDWALL}} \qquad (8)$$

where $q_{PROTECTEDWALL}$ is the mean overtopping discharge measured when the seawall is protected by rubble mounds (S-RMB and S-LCB), while $q_{UNPROTECTEDWALL}$ refers to the measurements obtained with the sole vertical wall as defence structure (*UP*).

The overtopping reduction offered by these protective structures is somehow due to their energy dissipation power, which their transmission coefficient, K_T, can globally represent. Furthermore, the analysis of these laboratory experiments also indicates that the structure's shallowness condition (i.e. $h_{TOE}/H_{m0,deep}$) plays a role in the flow rate reduction. Therefore, we relate the overtopping reduction ratio to a sort of modified Hofland et al.'s parameter, which is:

$$\frac{H_{m0,d,T}}{h_{TOE}} = K_T \cdot \frac{H_{m0,deep}}{h_{TOE}} \qquad (9)$$

where h_{TOE} refers to the water depth at the toe of the vertical wall, while K_T represents the effect of the protective structure accounting for all their geometrical features.

In Eq. 9, the transmission coefficient is determined via the Buccino and Calabrese (2007) formula, which has been derived for a wide range of crown widths and crest freeboards. Differently from previous applications of Buccino and Calabrese's equation, in this work we derive K_T using the deep water wave conditions to be consistent with the Hofland et al.'s parameter.

For both *S-RMB* and *S-LCB* data, results are plotted in Fig. 7. Numerical outcomes are plotted as well. It is worth specifying that, unlike the laboratory data, CFD experiments have been only performed with the seawall protected by RMBs. For determining C_q (Eq. 8), $q_{UNPROTECTEDWALL}$ has been obtained from a regression formula that relates q and $H_{m0,deep}$. The latter was developed by Di Leo (2021) by performing a wide CFD numerical experimental campaign on wave overtopping at the Malecòn seawall (Fig. 1).

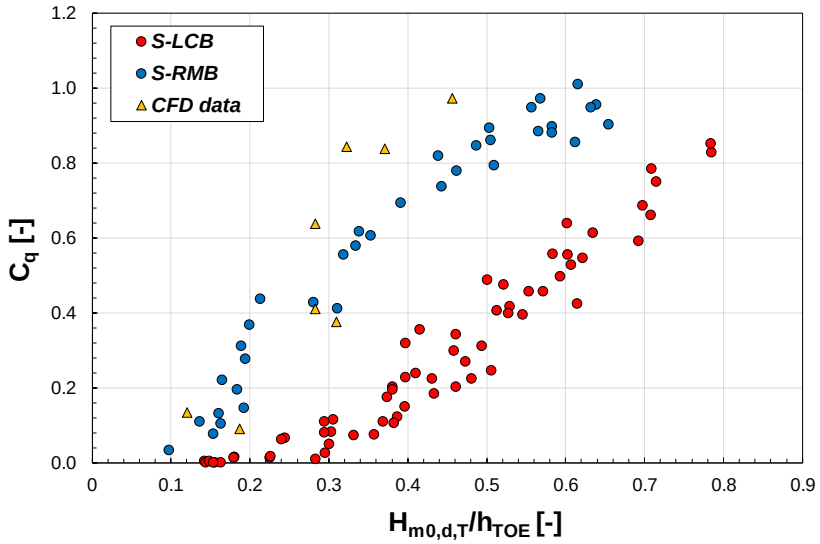

Figure 7. Wave overtopping reduction ratio vs the modified Hofland et al.'s parameter.

For each configuration, the laboratory data follow a clear trend that confirms the good explanatory power of Eq. 9. These trends indicate that the overtopping reduction capacity of rubble mound structures diminishes as the modified Hofland et al.'s parameter increases. Specifically, results in Fig. 7 suggest that, for a given structure (i.e., for a given K_T), the protective function weakens as the seawall is located in the deeper surf zone.

Numerical results (triangle points in Fig. 7) are fairly consistent with *S-RMB* laboratory experiments. Even though CFD data lies slightly above the laboratory ones for higher values of $H_{m0,d,T}/h_{TOE}$ – apparently following a relatively steeper trend – they confirm the validity of such a relationship.

Finally, it is worth noticing that the comparison between *S-RMB* and *S-LCB* data points out that protecting a seawall with a detached breakwater is a more efficient adaptive solution compared to the seawall protected by attached rubble mounds. *S-LCB* data indeed lie quite below *S-RMB* points.

Predictive tools

Based on these two trends, we have developed two predictive equations (Fig. 8). Specifically, Eq. 10 predicts the wave overtopping reduction ratio for seawalls protected by rubble mound breakwaters, while Eq. 11 can be used for estimating C_q of vertical walls protected by detached rubble mound structures. Such empirical predictive models read:

$$C_q = \frac{1}{\left[1 + 45 \cdot \exp\left(-13 \frac{H_{m0,d,T}}{h_{TOE}}\right)\right]} \qquad (10)$$

$$C_q = \frac{1}{\left[1 + 120 \cdot \exp\left(-8.2 \frac{H_{m0,d,T}}{h_{TOE}}\right)\right]} \qquad (11)$$

As discussed in the previous paragraph, Eqs. 10 and 11 consider that the reduction in wave overtopping tends to vanish when the sea defence is located in the inner surf zone.

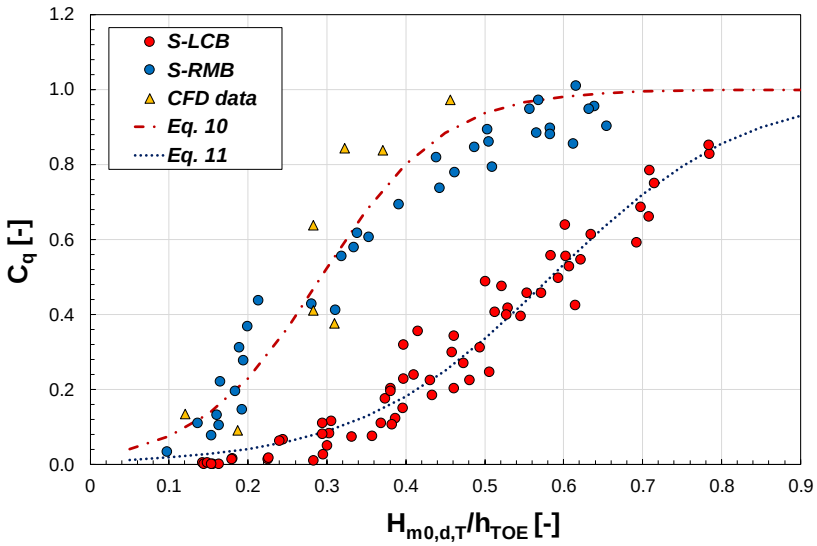

Figure 8. New predictive empirical equations.

Eqs. 10 and 11 may be helpful tools for designing adaptive sea defence configurations. Indeed, engineers can easily estimate the mean overtopping discharge by combining such empirical formulae and an overtopping model for vertical seawalls (e.g. EurOtop 2018).

Hence, we have verified these design tools using the CFD tests. In particular, we have coupled Eq. 10 along with two recent empirical formulae for wave overtopping of seawalls with very shallow foreshores, namely Lashley et al. (2021) and Tuozzo et al. (2024). The former is a deep-water-based model that relates q to deep water wave conditions, while the second requires wave set-up and wave

energy at the toe of the wall. The latter variables have been obtained by performing CFD wave propagation tests (i.e. without the structures in the numerical flume). Moreover, for both these empirical formulae, the flow rate also depends on the foreshore slope. As these experiments have been carried out on the multi-slope Havana foreshore (Fig. 1a), we use the equivalent slope proposed by Lashley et al. (2023) to estimate $q_{UNPROTECTEDWALL}$ via Lashley et al. (2021), whereas Tuozzo et al. (2024) suggested an averaged slope on twice the local wavelength for applying the overtopping predictive model in case of uneven bottoms. Finally, it is worth mentioning that Lashley et al.'s formula is valid for $h_{TOE}/H_{m0,deep} \leq 1$; thus, for larger values, we have used the EurOtop model for vertical walls, as suggested by the authors.

Fig. 9 compares q measured during numerical experiments and q computed using Eq. 10.

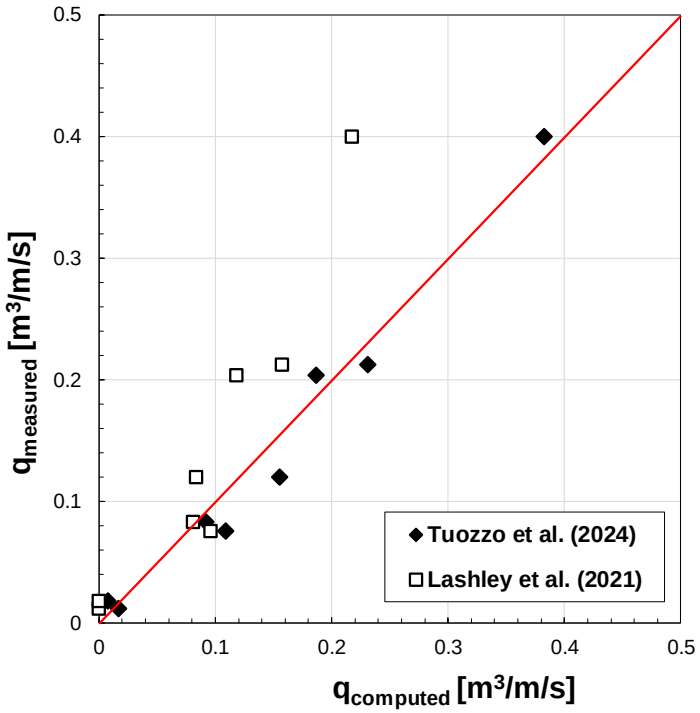

Figure 9. CFD data vs *q* computed using Eq. 10 and two different overtopping models for vertical walls. The red line represents the perfect agreement line.

Although we are evaluating a few data, the result shown in Fig. 9 is rather promising. The data indeed lie quite close to the perfect agreement line. This corroborates the capability of the predictive tool to estimate the reduction in the overtopping rate due to the presence of a protective structure.

Therefore, engineers can easily predict the mean overtopping discharge of seawalls protected by rubble mound structures by combining Eq. 10 (or Eq. 11) and an overtopping formula for vertical walls. Finally, it is worth noticing that, among the two formulae used in Fig. 9, Tuozzo et al.'s model provides more consistent results.

CONCLUSIONS

The present work dealt with the wave overtopping of vertical seawalls in shallow water conditions protected by either attached or detached rubble mound breakwaters.

We examined the laboratory data from a broad physical experimental campaign conducted at the University of Naples Federico II, along with numerical data from CFD experiments. The latter have been performed at the prototype scale using the technique proposed by Dentale et al. (2014a,b) to model porous structures.

Analyzing laboratory and numerical data, we related the capability of protective rubble mound structures in reducing wave overtopping at seawall to the transmitted deep water wave height to local water depth ratio ($H_{m0,d,T}/h_{TOE}$, i.e. the so-called modified Hofland et al. parameter); clearly, the transmitted wave height take into account the role of protective structure through their transmission coefficient. However, results pointed out an interesting behavior: these protective rubble mound structures seem to reduce the flow rate at the seawall as long as it is not located in the inner surf zone.

Based on these findings, we proposed two empirical tools for estimating the overtopping reduction ratio for seawalls protected by either rubble mound breakwaters or detached low-crested breakwaters. Coupling these formulae with an overtopping model for vertical walls may represent a helpful tool for coastal engineers to predict the mean overtopping discharge of seawalls protected by rubble mounds, as shown in Fig. 9.

Finally, the comparison between *S-RMB* and *S-LCB* experiments revealed that detached breakwaters have a more significant effect in reducing wave overtopping at seawalls compared to attached structures.

Future research will exploit the ability of the CFD numerical modelling to properly reproduce this phenomenon to extend and deepen our knowledge about the rule of rubble mound structures in mitigating the flooding risk of coastal areas.

REFERENCES

Buccino, M., and M. Calabrese. 2007. Conceptual approach for prediction of wave transmission at low-crested breakwaters. *Journal of waterway, port, coastal, and ocean engineering*, 133(3), 213-224.

Buccino, M.; Daliri, M., Calabrese, M., and R. Somma. 2021. A numerical study of arsenic contamination at the Bagnoli bay seabed by a semi-anthropogenic source. Analysis of current regime. *Science of the Total Environment*, 782,146811

Buccino, M., Di Leo, A., Tuozzo, S., Lopez, L.F.C., Calabrese, M., and F. Dentale. 2023. Wave overtopping of a vertical seawall in a surf zone: a joint analysis of numerical and laboratory data. *Ocean Engineering*, 288, 116144.

Calabrese, M., Vicinanza, D., and M. Buccino. 2008. 2D Wave setup behind submerged breakwaters. *Ocean Engineering*, *35*(10), 1015-1028.

Castellino, M., Romano, A., Lara, J.L., Losada, I.J., and P. de Girolamo. 2021. Confined-crest impact: forces dimensional analysis and extension of the Goda's formulae to recurved parapets. *Coastal Engineering*, 163

Chen, W., Warmink, J.J., Van Gent, M.R.A., and S.J.M.H. Hulscher. 2022. Numerical investigation of the effects of roughness, a berm and oblique waves on wave overtopping processes at dikes. *Applied Ocean Research*, 118

Dentale, F., Donnarumma, G., and E. Pugliese Carratelli, 2014a. Numerical wave interaction with tetrapods breakwater. *International journal of naval architecture and ocean engineering*, 6(4), 800-812.

Dentale, F., Donnarumma, G., and E. Pugliese Carratelli, 2014b. Simulation of flow within armour blocks in a breakwater. *Journal of coastal research*, 30(3), 528-536.

Di Leo, A., Reale, F., Dentale, F., Viccione, G., and E. Pugliese Carratelli. 2017. Wave-structure interactions a 2d innovative numerical methodology. In *Proceedings of the 23rd Conference of the Italian Association of Theoretical and Applied Mechanics*, 2, 1699-1708.

Di Leo, A. 2021. CFD Analysis of Coastal Flood Risk: Overtopping Related Phenomena. *Ph.D. Thesis*.

Di Leo, A., Dentale, F., Buccino, M., Tuozzo, S., and E. Pugliese Carratelli. 2022a. Numerical analysis of wind effect on wave overtopping on a vertical seawall. *Water*, 14(23), 3891.

Di Leo, A., Buccino, M., Dentale, F., E. Pugliese Carratelli. 2022b. CFD Analysis of Wind Effect on Wave Overtopping. In *Proceedings of the 32nd International Ocean and Polar Engineering Conference*, June 2022.

Dong, S., Salauddin, M., Abolfathi, S., and J. Pearson. 2021. Wave impact loads on vertical seawalls: Effects of the geometrical properties of recurve retrofitting. *Water*, 13(20), 2849.

EurOtop, Van der Meer, J.W., Allsop, N.W.H., Bruce, T., De Rouck, J., Kortenhaus, A., and T. Pullen. 2018. Manual on Wave Overtopping of Sea Defences and Related Structures. An overtopping Manual Largely Based On European research, but for Worldwide Application. Schüttrumpf.

Flow Science, Inc. 2009. FLOW-3D user's manual, HYDRO edition, Flow Science, Inc., Santa Fe, N.M.

Higuera, P., Lara, J. L., and I. J. Losada 2014. Three-dimensional interaction of waves and porous coastal structures using OpenFOAM®. Part I: Formulation and validation. *Coastal Engineering*, 83, 243-258.

Hofland, B., Chen, X., Altomare, C., and P. Oosterlo. 2017. Prediction formula for the spectral wave period Tm-1,0 on mildly sloping shallow foreshores. *Coastal Engineering*, 123, 21–28

Lashley, C.H., van der Meer, J.W., Bricker, J.D., Altomare, C., Suzuki, T., and K. Hirayama. 2021. Formulating wave overtopping at vertical and sloping structures with shallow foreshores using deep-water wave characteristics. *Journal Waterway Port Coastal Ocean Engineering*, 147, 6.

Lashley, C.H., Brown, J.M., Yelland, M.J., Van der Meer, J.W., and T. Pullen. 2023. Comparison of deep-water-parameter-based wave overtopping with wirewall field measurements and social media reports at Crosby (UK). *Coastal Engineering*, 179, 104241

Lin, P., and P. L. F. Liu. 1999. Internal wave-maker for Navier-Stokes equations models. *Journal of Waterway, Port, Coastal, and Ocean Engineering*, 125(4), 207-215.

Lopez, L. F. C., Salerno, D., Dentale, F., Capobianco, A., and M. Buccino. 2015. Experimental campaign on the overtopping of the seawall Malecòn Tradicional. In *the Twenty-fifth International Ocean and Polar Engineering Conference*, 2015

Lopez, C.L. F., Salerno, D., Dentale, F., Capobianco, A. and M. Buccino. 2016. Wave overtopping at Malecòn tradicional, La Habana, Cuba. *Proceedings of 34th International Conference on Coastal Engineering*, ASCE, 24-24.

Mata, M. I., and M. R. van Gent. 2023. Numerical modelling of wave overtopping discharges at rubble mound breakwaters using OpenFOAM®. *Coastal Engineering*, 181, 104274.

Pratola, L., Rinaldi, A., Molfetta, M. G., Bruno, M. F., Pasquali, D., Dentale, F., and M. Mossa. 2021. Investigation on the reflection coefficient for seawalls protected by a rubble mound structure. *Journal of Marine science and Engineering*, 9(9), 937.

Salauddin, M., O'Sullivan, J. J., Abolfathi, S., and J. M. Pearson. 2021. Eco-engineering of seawalls—an opportunity for enhanced climate resilience from increased topographic complexity. *Frontiers in Marine Science*, *8*, 674630.

Tuozzo, S., Calabrese, M., and M. Buccino. 2024. An overtopping formula for shallow water vertical seawalls by SWASH. *Applied Ocean Research*, 148, 104009.

Van Gent, M. R., Wolters, G., and A. Capel. 2022. Wave overtopping discharges at rubble mound breakwaters including effects of a crest wall and a berm. *Coastal Engineering*, 176, 104151.

Van Gent, M.R. 2024. Submerged low-crested structures in front of coastal structures. *Journal of Coastal and Hydraulic Structures*, 4, 33.

Zanuttigh, B., Formentin, S., and J.W. Van der Meer. 2016. Prediction of extreme and tolerable wave overtopping discharges through an advanced neural network. *Ocean Engineering*, 127, 722.